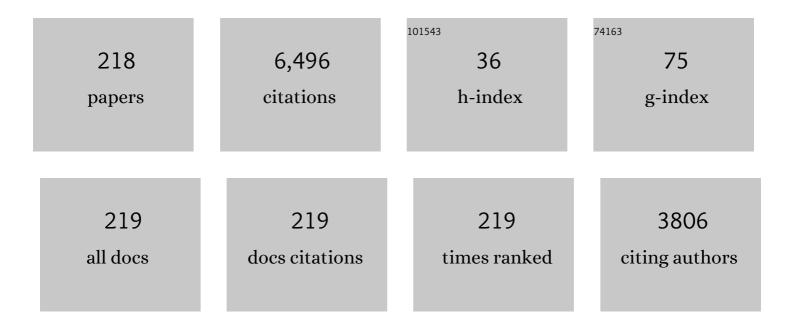
List of Publications by Year in descending order

Source: https://exaly.com/author-pdf/5196897/publications.pdf Version: 2024-02-01



HENCYONC YU

#	Article	IF	CITATIONS
1	Low-Dose CT Image Denoising Using a Generative Adversarial Network With Wasserstein Distance and Perceptual Loss. IEEE Transactions on Medical Imaging, 2018, 37, 1348-1357.	8.9	983
2	Low-Dose X-ray CT Reconstruction via Dictionary Learning. IEEE Transactions on Medical Imaging, 2012, 31, 1682-1697.	8.9	494
3	Compressed sensing based interior tomography. Physics in Medicine and Biology, 2009, 54, 2791-2805.	3.0	458
4	Convolutional Neural Network Based Metal Artifact Reduction in X-Ray Computed Tomography. IEEE Transactions on Medical Imaging, 2018, 37, 1370-1381.	8.9	300
5	An outlook on xâ€ray CT research and development. Medical Physics, 2008, 35, 1051-1064.	3.0	218
6	Multi-energy CT based on a prior rank, intensity and sparsity model (PRISM). Inverse Problems, 2011, 27, 115012.	2.0	191
7	A soft-threshold filtering approach for reconstruction from a limited number of projections. Physics in Medicine and Biology, 2010, 55, 3905-3916.	3.0	176
8	A General Local Reconstruction Approach Based on a Truncated Hilbert Transform. International Journal of Biomedical Imaging, 2007, 2007, 1-8.	3.9	136
9	Tensor-Based Dictionary Learning for Spectral CT Reconstruction. IEEE Transactions on Medical Imaging, 2017, 36, 142-154.	8.9	131
10	High-order total variation minimization for interior tomography. Inverse Problems, 2010, 26, 035013.	2.0	115
11	Low-dose spectral CT reconstruction using image gradient ℓ0–norm and tensor dictionary. Applied Mathematical Modelling, 2018, 63, 538-557.	4.2	115
12	DRONE: Dual-Domain Residual-based Optimization NEtwork for Sparse-View CT Reconstruction. IEEE Transactions on Medical Imaging, 2021, 40, 3002-3014.	8.9	101
13	Tensor-based dictionary learning for dynamic tomographic reconstruction. Physics in Medicine and Biology, 2015, 60, 2803-2818.	3.0	99
14	A Segmentation-Based Method for Metal Artifact Reduction. Academic Radiology, 2007, 14, 495-504.	2.5	93
15	A general exact reconstruction for cone-beam CT via backprojection-filtration. IEEE Transactions on Medical Imaging, 2005, 24, 1190-1198.	8.9	89
16	Image Reconstruction for Hybrid True-Color Micro-CT. IEEE Transactions on Biomedical Engineering, 2012, 59, 1711-1719.	4.2	81
17	Statistical Interior Tomography. IEEE Transactions on Medical Imaging, 2011, 30, 1116-1128.	8.9	77
18	The meaning of interior tomography. Physics in Medicine and Biology, 2013, 58, R161-R186.	3.0	75

#	Article	IF	CITATIONS
19	A General-Thresholding Solution for l <sub>p</sub> (0 <; p <; 1) Regularized CT Reconstruction. IEEE Transactions on Image Processing, 2015, 24, 5455-5468.	9.8	72
20	Data Consistency Based Rigid Motion Artifact Reduction in Fan-Beam CT. IEEE Transactions on Medical Imaging, 2007, 26, 249-260.	8.9	70
21	Ultra-low Dose Lung CT Perfusion Regularized by a Previous Scan. Academic Radiology, 2009, 16, 363-373.	2.5	68
22	Supplemental analysis on compressed sensing based interior tomography. Physics in Medicine and Biology, 2009, 54, N425-N432.	3.0	59
23	Machine learning-enabled non-destructive paper chromogenic array detection of multiplexed viable pathogens on food. Nature Food, 2021, 2, 110-117.	14.0	54
24	Non-Local Low-Rank Cube-Based Tensor Factorization for Spectral CT Reconstruction. IEEE Transactions on Medical Imaging, 2019, 38, 1079-1093.	8.9	52
25	CLEAR: Comprehensive Learning Enabled Adversarial Reconstruction for Subtle Structure Enhanced Low-Dose CT Imaging. IEEE Transactions on Medical Imaging, 2021, 40, 3089-3101.	8.9	52
26	A unified framework for exact cone-beam reconstruction formulas. Medical Physics, 2005, 32, 1712-1721.	3.0	51
27	Exact Interior Reconstruction from Truncated Limited-Angle Projection Data. International Journal of Biomedical Imaging, 2008, 2008, 1-6.	3.9	51
28	Approximate and exact cone-beam reconstruction with standard and non-standard spiral scanning. Physics in Medicine and Biology, 2007, 52, R1-R13.	3.0	49
29	Exact Interior Reconstruction with Cone-Beam CT. International Journal of Biomedical Imaging, 2007, 2007, 1-5.	3.9	49
30	A scheme for multisource interior tomography. Medical Physics, 2009, 36, 3575-3581.	3.0	49
31	Sart-Type Half-Threshold Filtering Approach for CT Reconstruction. IEEE Access, 2014, 2, 602-613.	4.2	49
32	Data consistency based translational motion artifact reduction in fan-beam CT. IEEE Transactions on Medical Imaging, 2006, 25, 792-803.	8.9	48
33	Interior Reconstruction Using the Truncated Hilbert Transform via Singular Value Decomposition. Journal of X-Ray Science and Technology, 2008, 16, 243-251.	1.0	41
34	Metalnv-Net: Meta Inversion Network for Sparse View CT Image Reconstruction. IEEE Transactions on Medical Imaging, 2021, 40, 621-634.	8.9	39
35	A backprojection-filtration algorithm for nonstandard spiral cone-beam CT with ann-PI-window. Physics in Medicine and Biology, 2005, 50, 2099-2111.	3.0	38
36	Towards Omni-Tomography—Grand Fusion of Multiple Modalities for Simultaneous Interior Tomography. PLoS ONE, 2012, 7, e39700.	2.5	38

#	Article	IF	CITATIONS
37	Non-uniqueness and instability of â€~ankylography'. Nature, 2011, 480, E2-E3.	27.8	36
38	Exact BPF and FBP algorithms for nonstandard saddle curves. Medical Physics, 2005, 32, 3305-3312.	3.0	35
39	Design, analysis and simulation for development of the first clinical micro-CT scanner1. Academic Radiology, 2005, 12, 511-525.	2.5	35
40	A General Total Variation Minimization Theorem for Compressed Sensing Based Interior Tomography. International Journal of Biomedical Imaging, 2009, 2009, 1-3.	3.9	33
41	SART-Type Image Reconstruction from a Limited Number of Projections with the Sparsity Constraint. International Journal of Biomedical Imaging, 2010, 2010, 1-9.	3.9	33
42	Feldkamp-type VOI reconstruction from super-short-scan cone-beam data. Medical Physics, 2004, 31, 1357-1362.	3.0	30
43	Finite detector based projection model for high spatial resolution. Journal of X-Ray Science and Technology, 2012, 20, 229-238.	1.0	30
44	Improved Material Decomposition With a Two-Step Regularization for Spectral CT. IEEE Access, 2019, 7, 158770-158781.	4.2	30
45	Spatial-spectral cube matching frame for spectral CT reconstruction. Inverse Problems, 2018, 34, 104003.	2.0	29
46	Spectral CT Reconstruction—ASSIST: Aided by Self-Similarity in Image-Spectral Tensors. IEEE Transactions on Computational Imaging, 2019, 5, 420-436.	4.4	29
47	Local ROI Reconstruction via Generalized FBP and BPF Algorithms along More Flexible Curves. International Journal of Biomedical Imaging, 2006, 2006, 1-7.	3.9	28
48	Low-dose spectral CT reconstruction based on image-gradient L <sub>0</sub> -norm and adaptive spectral PICCS. Physics in Medicine and Biology, 2020, 65, 245005.	3.0	28
49	Image reconstruction from limited angle projections collected by multisource interior x-ray imaging systems. Physics in Medicine and Biology, 2011, 56, 6337-6357.	3.0	24
50	Hybrid Spectral Micro-CT: System Design, Implementation, and Preliminary Results. IEEE Transactions on Biomedical Engineering, 2014, 61, 246-253.	4.2	24
51	Swinging multi-source industrial CT systems for aperiodic dynamic imaging. Optics Express, 2017, 25, 24215.	3.4	24
52	Nondestructive multiplex detection of foodborne pathogens with background microflora and symbiosis using a paper chromogenic array and advanced neural network. Biosensors and Bioelectronics, 2021, 183, 113209.	10.1	24
53	Exact reconstruction for cone-beam scanning along nonstandard spirals and other curves. , 2004, , .		23
54	A differentiable Shepp–Logan phantom and its applications in exact cone-beam CT. Physics in Medicine and Biology, 2005, 50, 5583-5595.	3.0	23

#	Article	lF	CITATIONS
55	Compressive Sensing–Based Interior Tomography. Journal of Computer Assisted Tomography, 2011, 35, 762-764.	0.9	23
56	High-order total variation minimization for interior SPECT. Inverse Problems, 2012, 28, 015001.	2.0	23
57	Scout-view assisted interior micro-CT. Physics in Medicine and Biology, 2013, 58, 4297-4314.	3.0	23
58	Completeness map evaluation demonstrated with candidate nextâ€generation cardiac CT architectures. Medical Physics, 2012, 39, 2405-2416.	3.0	22
59	An adaptive reconstruction algorithm for spectral CT regularized by a reference image. Physics in Medicine and Biology, 2016, 61, 8699-8719.	3.0	22
60	TED-Net: Convolution-Free T2T Vision Transformer-Based Encoder-Decoder Dilation Network for Low-Dose CTÂDenoising. Lecture Notes in Computer Science, 2021, , 416-425.	1.3	22
61	GPU-Based Branchless Distance-Driven Projection and Backprojection. IEEE Transactions on Computational Imaging, 2017, 3, 617-632.	4.4	21
62	Locally linear constraint based optimization model for material decomposition. Physics in Medicine and Biology, 2017, 62, 8314-8340.	3.0	21
63	Diffractive Elements for Zero-Order Bessel Beam Generation With Application in the Terahertz Reflection Imaging. IEEE Photonics Journal, 2019, 11, 1-12.	2.0	21
64	Katsevich-type algorithims for variable radius spiral cone-beam CT. , 2004, , .		20
65	A Parallel Implementation of the Katsevich Algorithm for 3-D CT Image Reconstruction. Journal of Supercomputing, 2006, 38, 35-47.	3.6	20
66	Compressive sampling based interior reconstruction for dynamic carbon nanotube micro-CT. Journal of X-Ray Science and Technology, 2009, 17, 295-303.	1.0	20
67	Spectrum Estimation-Guided Iterative Reconstruction Algorithm for Dual Energy CT. IEEE Transactions on Medical Imaging, 2020, 39, 246-258.	8.9	20
68	Image-Domain Material Decomposition for Spectral CT Using a Generalized Dictionary Learning. IEEE Transactions on Radiation and Plasma Medical Sciences, 2021, 5, 537-547.	3.7	20
69	Interior SPECT—exact and stable ROI reconstruction from uniformly attenuated local projections. Communications in Numerical Methods in Engineering, 2009, 25, 693-710.	1.3	19
70	Interior Tomography With Continuous Singular Value Decomposition. IEEE Transactions on Medical Imaging, 2012, 31, 2108-2119.	8.9	18
71	Experimental studies on few-view reconstruction for high-resolution micro-CT. Journal of X-Ray Science and Technology, 2013, 21, 25-42.	1.0	17
72	Interior micro T with an offset detector. Medical Physics, 2014, 41, 061915.	3.0	17

#	Article	IF	CITATIONS
73	Cone-beam pseudo-lambda tomography. Inverse Problems, 2007, 23, 203-215.	2.0	16
74	Experimental measurement of human head motion for high-resolution computed tomography system design. Optical Engineering, 2010, 49, 063201.	1.0	16
75	Correlation coefficient based supervised locally linear embedding for pulmonary nodule recognition. Computer Methods and Programs in Biomedicine, 2016, 136, 97-106.	4.7	16
76	Review of CT image reconstruction open source toolkits. Journal of X-Ray Science and Technology, 2020, 28, 619-639.	1.0	16
77	MD-NDNet: a multi-dimensional convolutional neural network for false-positive reduction in pulmonary nodule detection. Physics in Medicine and Biology, 2020, 65, 235053.	3.0	16
78	Stabilizing deep tomographic reconstruction: Part A. Hybrid framework and experimental results. Patterns, 2022, 3, 100474.	5.9	16
79	BPF-type region-of-interest reconstruction for parallel translational computed tomography. Journal of X-Ray Science and Technology, 2017, 25, 487-504.	1.0	15
80	Block matching frame based material reconstruction for spectral CT. Physics in Medicine and Biology, 2019, 64, 235011.	3.0	15
81	Studies on artifacts of the Katsevich algorithm for spiral cone-beam CT. , 2004, , .		14
82	Practical cone-beam lambda tomography. Medical Physics, 2006, 33, 3640-3646.	3.0	14
83	Dictionary learning based image-domain material decomposition for spectral CT. Physics in Medicine and Biology, 2020, 65, 245006.	3.0	14
84	MSANet: Multiscale Aggregation Network Integrating Spatial and Channel Information for Lung Nodule Detection. IEEE Journal of Biomedical and Health Informatics, 2022, 26, 2547-2558.	6.3	14
85	Integral Invariants for Computed Tomography. IEEE Signal Processing Letters, 2006, 13, 549-552.	3.6	13
86	Tensor decomposition and non-local means based spectral CT image denoising. Journal of X-Ray Science and Technology, 2019, 27, 397-416.	1.0	13
87	Image gradient L <sub>0</sub> -norm based PICCS for swinging multi-source CT reconstruction. Optics Express, 2019, 27, 5264.	3.4	13
88	Stabilizing deep tomographic reconstruction: Part B. Convergence analysis and adversarial attacks. Patterns, 2022, 3, 100475.	5.9	13
89	Can interior tomography outperform lambda tomography?. Proceedings of the National Academy of Sciences of the United States of America, 2010, 107, E92-3, author reply E94-5.	7.1	12
90	Energy-discriminative performance of a spectral micro-CT system. Journal of X-Ray Science and Technology, 2013, 21, 335-345.	1.0	12

#	Article	IF	CITATIONS
91	A Stationary-Sources and Rotating-Detectors Computed Tomography Architecture for Higher Temporal Resolution and Lower Radiation Dose. IEEE Access, 2014, 2, 1263-1271.	4.2	12
92	Pseudo progression identification of glioblastoma with dictionary learning. Computers in Biology and Medicine, 2016, 73, 94-101.	7.0	12
93	A family of analytic algorithms for cone-beam CT. , 2004, , .		11
94	The impact of calibration phantom errors on dual-energy digital mammography. Physics in Medicine and Biology, 2008, 53, 6321-6336.	3.0	11
95	An improved distance-driven method for projection and backprojection. Journal of X-Ray Science and Technology, 2014, 22, 1-18.	1.0	11
96	Iterative spectral CT reconstruction based on low rank and average-image-incorporated BM3D. Physics in Medicine and Biology, 2018, 63, 155021.	3.0	11
97	A General Formula for Fan-Beam Lambda Tomography. International Journal of Biomedical Imaging, 2006, 2006, 1-9.	3.9	10
98	A General Formula for Fan-Beam Lambda Tomography (Erratum). International Journal of Biomedical Imaging, 2007, 2007, 1-1.	3.9	10
99	Data consistency condition–based beam-hardening correction. Optical Engineering, 2011, 50, 076501.	1.0	10
100	Preliminary experimental results from a MARS Micro-CT system. Journal of X-Ray Science and Technology, 2012, 20, 199-211.	1.0	10
101	GPU-Based Acceleration for Interior Tomography. IEEE Access, 2014, 2, 757-770.	4.2	10
102	Cone-beam mammo-computed tomography from data along two tilting arcs. Medical Physics, 2006, 33, 3621-3633.	3.0	9
103	Gel'fand-Graev's reconstruction formula in the 3D real space. Medical Physics, 2011, 38, S69-S75.	3.0	9
104	Alternating Iteration for <inline-formula> <tex-math notation="LaTeX">\$l_{p}\$ </tex-math> </inline-formula> ( <inline-formula> <tex-math) 0="" 10="" etqq0="" overlock="" rgbt="" td="" tf<="" tj=""><td>50,222 To 4.2</td><td>d (notation="</td></tex-math)></inline-formula>	50,222 To 4.2	d (notation="
105	Reconstruction. IEEE Access, 2016, 4, 4355-4363. Lambda tomography with discontinuous scanning trajectories. Physics in Medicine and Biology, 2007, 52, 4331-4344.	3.0	8
106	Top-level design and pilot analysis of low-end CT scanners based on linear scanning for developing countries. Journal of X-Ray Science and Technology, 2014, 22, 673-686.	1.0	8
107	Dictionaryâ€learningâ€based reconstruction method for electron tomography. Scanning, 2014, 36, 377-383.	1.5	8
108	Guest Editorial Special Issue on Spectral CT. IEEE Transactions on Medical Imaging, 2015, 34, 693-696.	8.9	8

#	Article	IF	CITATIONS
109	Interior tomography with curvelet-based regularization. Journal of X-Ray Science and Technology, 2017, 25, 1-13.	1.0	8
110	Sparse-Prior-Based Projection Distance Optimization Method for Joint CT-MRI Reconstruction. IEEE Access, 2017, 5, 20099-20110.	4.2	8
111	Spectral CT Reconstruction Based on PICCS and Dictionary Learning. IEEE Access, 2020, 8, 133367-133376.	4.2	8
112	CT imaging of gold nanoparticles in a humanâ€sized phantom. Journal of Applied Clinical Medical Physics, 2021, 22, 337-342.	1.9	8
113	A beam hardening correction method based on HL consistency. , 2006, 6318, 583.		7
114	Comparison on beam hardening correction of CT based on H-L consistency and normal water phantom experiment. , 2006, , .		7
115	Demonstration of Dose and Scatter Reductions for Interior Computed Tomography. Journal of Computer Assisted Tomography, 2009, 33, 967-972.	0.9	7
116	Fast Exact/Quasi-Exact FBP Algorithms for Triple-Source Helical Cone-Beam CT. IEEE Transactions on Medical Imaging, 2010, 29, 756-770.	8.9	7
117	Statistical interior tomography. Proceedings of SPIE, 2010, , .	0.8	7
118	SART-Type Image Reconstruction from Overlapped Projections. International Journal of Biomedical Imaging, 2011, 2011, 1-7.	3.9	7
119	A new iterative algorithm for ring artifact reduction in CT using ring total variation. Medical Physics, 2019, 46, 4803-4815.	3.0	7
120	Cone-Beam Composite-Circling Scan and Exact Image Reconstruction for a Quasi-Short Object. International Journal of Biomedical Imaging, 2007, 2007, 1-10.	3.9	6
121	Parallelism of iterative CT reconstruction based onÂlocal reconstruction algorithm. Journal of Supercomputing, 2009, 48, 1-14.	3.6	6
122	Dictionary Learning Based Low-Dose X-Ray CT Reconstruction. , 2014, , 99-119.		6
123	Issue Information. Scanning, 2014, 36, 377-83.	1.5	6
124	Dictionary learning based low-dose x-ray CT reconstruction using a balancing principle. , 2014, , .		6
125	Interior tomographic imaging of mouse heart in a carbon nanotube micro-CT. Journal of X-Ray Science and Technology, 2016, 24, 549-563.	1.0	6
126	Comparison Study of Regularizations in Spectral Computed Tomography Reconstruction. Sensing and Imaging, 2018, 19, 1.	1.5	6

HENGYONG YU

#	Article	IF	CITATIONS
127	Optimization of Energy Combination for Gold-Based Contrast Agents Below <inline-formula> <tex-math notation="LaTeX">\${K}\$ </tex-math> </inline-formula> -Edges in Dual-Energy Micro-CT. IEEE Transactions on Radiation and Plasma Medical Sciences, 2018, 2, 187-193.	3.7	6
128	Theoretically exact backprojection filtration algorithm for multi-segment linear trajectory. Physics in Medicine and Biology, 2018, 63, 015037.	3.0	6
129	Multiscale Tensor Dictionary Learning Approach for Multispectral Image Denoising. IEEE Access, 2018, 6, 51898-51910.	4.2	6
130	Studies on Palamodov's algorithm for cone-beam CT along a general curve. Inverse Problems, 2006, 22, 447-460.	2.0	5
131	Digital Tomosynthesis Aided by Low-Resolution Exact Computed Tomography. Journal of Computer Assisted Tomography, 2007, 31, 976-983.	0.9	5
132	A comparative study on interpolation methods for controlled cardiac CT. International Journal of Imaging Systems and Technology, 2007, 17, 91-98.	4.1	5
133	Beam hardening correction based on HL consistency in polychromatic transmission tomography. , 2008, , .		5
134	Cardiac Computed Tomography Radiation Dose Reduction Using Interior Reconstruction Algorithm With the Aorta and Vertebra as Known Information. Journal of Computer Assisted Tomography, 2009, 33, 338-347.	0.9	5
135	Analytic reconstruction approach for parallel translational computed tomography. Journal of X-Ray Science and Technology, 2015, 23, 213-228.	1.0	5
136	Relevance Vector Machine Based Pulmonary Nodule Classification. Journal of Medical Imaging and Health Informatics, 2016, 6, 163-169.	0.3	5
137	Cardiac CT: A system architecture study. Journal of X-Ray Science and Technology, 2016, 24, 43-65.	1.0	5
138	Adaptive Nonlocal Means Method for Denoising Basis Material Images From Dual-Energy Computed Tomography. Journal of Computer Assisted Tomography, 2018, 42, 972-981.	0.9	5
139	A spectral CT denoising algorithm based on weighted block matching 3D filtering. , 2017, , .		5
140	Reduction of metal artifacts in x-ray CT images using a convolutional neural network. , 2017, , .		5
141	Development of Computed Tomography Algorithms. International Journal of Biomedical Imaging, 2006, 2006, 1-3.	3.9	4
142	Line-Source Based X-Ray Tomography. International Journal of Biomedical Imaging, 2009, 2009, 1-8.	3.9	4
143	Compressed sensing based interior tomography. Physics in Medicine and Biology, 2009, 54, 4341-4341.	3.0	4
144	Data consistency condition for truncated projections in fan-beam geometry. Journal of X-Ray Science and Technology, 2015, 23, 627-638.	1.0	4

#	Article	IF	CITATIONS
145	Singular value decomposition-based 2D image reconstruction for computed tomography. Journal of X-Ray Science and Technology, 2017, 25, 113-134.	1.0	4
146	Locally linear transform based threeâ€dimensional gradient â€norm minimization for spectral CT reconstruction. Medical Physics, 2020, 47, 4810-4826.	3.0	4
147	Tensor Gradient Lâ,€-Norm Minimization-Based Low-Dose CT and Its Application to COVID-19. IEEE Transactions on Instrumentation and Measurement, 2021, 70, 1-12.	4.7	4
148	A directional TV based ring artifact reduction method. , 2019, , .		4
149	Fine-grained calibrated double-attention convolutional network for left ventricular segmentation. Physics in Medicine and Biology, 2022, 67, 055013.	3.0	4
150	A general scheme for velocity tomography. Signal Processing, 2008, 88, 1165-1175.	3.7	3
151	Interior tomography: theory, algorithms and applications. , 2008, , .		3
152	Knowledge-Based Dynamic Volumetric Cardiac Computed Tomography With Saddle Curve Trajectory. Journal of Computer Assisted Tomography, 2008, 32, 942-950.	0.9	3
153	Exact and stable interior ROI reconstruction for radial MRI. , 2009, , .		3
154	Multibeam field emission xâ€ray system with halfâ€scan reconstruction algorithm. Medical Physics, 2010, 37, 3773-3781.	3.0	3
155	Piecewise-Constant-Model-Based Interior Tomography Applied to Dentin Tubules. Computational and Mathematical Methods in Medicine, 2013, 2013, 1-8.	1.3	3
156	Tensor decomposition and nonlocal means based spectral CT reconstruction. , 2016, , .		3
157	Cardiac CT motion artifact grading via semi-automatic labeling and vessel tracking using synthetic image-augmented training data. Journal of X-Ray Science and Technology, 2022, 30, 433-445.	1.0	3
158	Numerical studies on Feldkamp-type and Katsevich-type algorithms for cone-beam scanning along nonstandard spirals. , 2004, , .		2
159	Analytic simulation scheme for x-ray projections based on physics model. , 2006, , .		2
160	Projection-based Bolus Detection for Computed Tomographic Angiography. Journal of Computer Assisted Tomography, 2006, 30, 846-849.	0.9	2
161	Reply to the comment on â€~Studies on Palamodov's algorithm for cone-beam CT along a general curve'. Inverse Problems, 2006, 22, 1505-1506.	2.0	2
162	Laplace operator based reconstruction algorithm for truncated spiral cone beam computed tomography. Journal of X-Ray Science and Technology, 2013, 21, 515-526.	1.0	2

#	Article	IF	CITATIONS
163	Analytic reconstruction algorithms for tripleâ€source CT with horizontal data truncation. Medical Physics, 2015, 42, 6062-6073.	3.0	2
164	Comparison studies of different regularizers for spectral computed tomography. , 2016, , .		2
165	Ordered-subset Split-Bregman algorithm for interior tomography. Journal of X-Ray Science and Technology, 2016, 24, 221-240.	1.0	2
166	Evaluation of an Analytic Reconstruction Method as a Platform for Spectral Cone-Beam CT. IEEE Access, 2018, 6, 21314-21323.	4.2	2
167	Wavelet-based joint CT-MRI reconstruction. Journal of X-Ray Science and Technology, 2018, 26, 379-393.	1.0	2
168	FBP-type CT reconstruction algorithms for triple-source circular trajectory with different scanning radii. Journal of X-Ray Science and Technology, 2019, 27, 665-684.	1.0	2
169	Tensor framelet based iterative image reconstruction algorithm for low-dose multislice helical CT. PLoS ONE, 2019, 14, e0210410.	2.5	2
170	Compton-camera-based SPECT for thyroid cancer imaging. Journal of X-Ray Science and Technology, 2021, 29, 111-124.	1.0	2
171	Robust Frame Based X-Ray CT Reconstruction. Journal of Computational Mathematics, 2016, 34, 683-704.	0.4	2
172	Generative Low-Dose CT Image Denoising. Advances in Computer Vision and Pattern Recognition, 2019, , 277-297.	1.3	2
173	Medipix-based Spectral Micro-CT. CT Lilun Yu Yingyong Yanjiu, 2012, 21, 583.	0.0	2
174	Haze Level Evaluation Using Dark and Bright Channel Prior Information. Atmosphere, 2022, 13, 683.	2.3	2
175	Skew cone beam lambda tomography. , 2006, , .		1
176	General formulation for X-ray computed tomography. , 2006, , .		1
177	Practical cone-beam lambda tomography. , 2006, , .		1
178	Determination of exact reconstruction regions in composite-circling cone-beam tomography. Medical Physics, 2009, 36, 3448-3454.	3.0	1
179	Scatter correction algorithm without extra exposure for dual-energy digital mammography. , 2009, , .		1
180	Adaptive beam hardening correction based on projection data consistency condition. , 2010, , .		1

11

#	Article	IF	CITATIONS
181	Recent progress in local reconstruction. , 2010, , .		1
182	CT gradient image reconstruction directly from projections. Journal of X-Ray Science and Technology, 2011, 19, 173-198.	1.0	1
183	Speedup performance analysis of parallel Katsevich algorithm for 3D CT image reconstruction. International Journal of Computational Science and Engineering, 2011, 6, 151.	0.5	1
184	High order total variation method for interior tomography. Proceedings of SPIE, 2012, , .	0.8	1
185	Stereo-imaging towards spectrography for 3D analysis from a single spectral view. , 2012, , .		1
186	A new CT architecture with stationary x-ray sources. Proceedings of SPIE, 2012, , .	0.8	1
187	Study of scan protocol for exposure reduction in hybrid spectral microâ€CT. Scanning, 2014, 36, 444-455.	1.5	1
188	Scalable 2D K-SVD parallel algorithm for dictionary learning on GPUs. , 2016, , .		1
189	Initial analysis of the middle problem in CT image reconstruction. Journal of X-Ray Science and Technology, 2017, 25, 547-559.	1.0	1
190	Refined Locally Linear Transform-Based Spectral-Domain Gradient Sparsity and Its Applications in Spectral CT Reconstruction. IEEE Access, 2021, 9, 58537-58548.	4.2	1
191	Refined locally linear transform based spectral-domain gradient sparsity and its applications in spectral CT reconstruction. , 2019, , .		1
192	Evaluation of GPU-Based CT Reconstruction for Morbidly Obese Patients. JSM Biomedical Imaging Data Papers, 2017, 4, .	0.0	1
193	Image reconstruction via truncated lambda tomography. , 2006, 6318, 491.		0
194	Geometrical study on two tilting arcs based exact cone-beam CT for breast imaging. , 2006, 6318, 509.		0
195	Deployment of One-Sided Communication Technique for Parallel Computing in Katsevich CT Image Reconstruction. , 2006, , .		0
196	Analysis of Performance Evaluation of Parallel Katsevich Algorithm for 3-D CT Image Reconstruction. , 2006, , .		0
197	Determination of the exact reconstruction region in the cone-beam composite-circling mode. , 2008, , .		0

A study on spiral cone beam scanning mode for preclinical micro-CT. , 2009, , .

0

#	Article	IF	CITATIONS
199	Interior tomography from low-count local projections and associated Hilbert transform data. , 2011, , .		0
200	Noise reduction by projection direction dependent diffusion for low dose fan-beam x-ray computed tomography. , 2011, , .		0
201	Inverse Fourier Transform in the Gamma Coordinate System. International Journal of Biomedical Imaging, 2011, 2011, 1-16.	3.9	0
202	An RIP-based evaluation method for candidate next generation cardiac CT architectures with carbon nanotube x-ray source. , 2012, , .		0
203	Spectrography: volumetric reconstruction from one or two spectral views. , 2012, , .		0
204	Spectrography for 3D analysis from a single spectral view. Proceedings of SPIE, 2013, , .	0.8	0
205	IEEE Access Special Section Editorial: Emerging Computed Tomography Technologies. IEEE Access, 2014, 2, 1680-1682.	4.2	0
206	Total variation minimization-based multimodality medical image reconstruction. , 2014, , .		0
207	Real phantom datasets for the evaluation of reconstruction algorithms at various dose conditions. , 2014, , .		0
208	Bisection and twisted SVD on GPU. , 2015, , .		0
209	Dictionary learning-based CT detection of pulmonary nodules. Proceedings of SPIE, 2016, , .	0.8	Ο
210	Locally Linear Embedding-Based Motion Estimation From Truncated Projections for Computed Tomography. IEEE Access, 2017, 5, 11155-11165.	4.2	0
211	Geometry and energy constrained projection extension. Journal of X-Ray Science and Technology, 2018, 26, 757-775.	1.0	0
212	Spectral Ct Reconstruction Via Self-Similarity In Image-Spectral Tensors. , 2019, , .		0
213	IEEE Access Special Section Editorial: Multi-Energy Computed Tomography and its Applications. IEEE Access, 2021, 9, 117303-117305.	4.2	Ο
214	A deep learning approach to gold nanoparticle quantification in computed tomography. Physica Medica, 2021, 87, 83-89.	0.7	0
215	Blind image quality evaluation using the conditional histogram patterns of divisive normalization transform coefficients. , 2017, , .		0
216	Multi-domain constraint based one-step selective-reconstruction method for spectral micro-CT. , 2018, , .		0

#	Article	IF	CITATIONS
217	ELDA. , 2020, , .		0
218	Automatic Patient-Level Detection of Coronavirus Disease (COVID-19) Using Convolutional Neural Network from Lung CT Scans. Journal of Medical Imaging and Health Informatics, 2021, 11, 2722-2732.	0.3	0